



HAL
open science

Bose-Einstein correlations in W-pair decays

R. Barate, D. Decamp, P. Ghez, C. Goy, S. Jezequel, J.P. Lees, F. Martin, E. Merle, M.N. Minard, B. Pietrzyk, et al.

► **To cite this version:**

R. Barate, D. Decamp, P. Ghez, C. Goy, S. Jezequel, et al.. Bose-Einstein correlations in W-pair decays. Physics Letters B, 2000, 478, pp.50-64. in2p3-00005332

HAL Id: in2p3-00005332

<https://hal.in2p3.fr/in2p3-00005332>

Submitted on 12 May 2000

HAL is a multi-disciplinary open access archive for the deposit and dissemination of scientific research documents, whether they are published or not. The documents may come from teaching and research institutions in France or abroad, or from public or private research centers.

L'archive ouverte pluridisciplinaire **HAL**, est destinée au dépôt et à la diffusion de documents scientifiques de niveau recherche, publiés ou non, émanant des établissements d'enseignement et de recherche français ou étrangers, des laboratoires publics ou privés.

Bose-Einstein correlations in W -pair decays

The ALEPH Collaboration

Abstract

Bose-Einstein correlations are studied in semileptonic ($WW \rightarrow q\bar{q}\ell\nu$) and fully hadronic ($WW \rightarrow q\bar{q}q\bar{q}$) W -pair decays with the ALEPH detector at LEP at centre-of-mass energies of 172, 183 and 189 GeV. They are compared with those made at the Z peak after correction for the different flavour compositions. A Monte Carlo model of Bose-Einstein correlations based on the JETSET hadronization scheme was tuned to the Z data and reproduces the correlations in the $WW \rightarrow q\bar{q}\ell\nu$ events. The same Monte Carlo reproduces the correlations in the $WW \rightarrow q\bar{q}q\bar{q}$ channel assuming independent fragmentation of the two W 's. A variant this model with Bose-Einstein correlations between decay products of different W 's is disfavoured.

Submitted to Physics Letters B

The ALEPH Collaboration

R. Barate, D. Decamp, P. Ghez, C. Goy, S. Jezequel, J.-P. Lees, F. Martin, E. Merle, M.-N. Minard, B. Pietrzyk

Laboratoire de Physique des Particules (LAPP), IN²P³-CNRS, F-74019 Annecy-le-Vieux Cedex, France

R. Alemany, S. Bravo, M.P. Casado, M. Chmeissani, J.M. Crespo, E. Fernandez, M. Fernandez-Bosman, Ll. Garrido,¹⁵ E. Graugés, A. Juste, M. Martinez, G. Merino, R. Miquel, Ll.M. Mir, P. Morawitz, A. Pacheco, I. Riu, H. Ruiz

Institut de Física d'Altes Energies, Universitat Autònoma de Barcelona, E-08193 Bellaterra (Barcelona), Spain⁷

A. Colaleo, D. Creanza, M. de Palma, G. Iaselli, G. Maggi, M. Maggi, S. Nuzzo, A. Ranieri, G. Raso, F. Ruggieri, G. Selvaggi, L. Silvestris, P. Tempesta, A. Tricomi,³ G. Zito

Dipartimento di Fisica, INFN Sezione di Bari, I-70126 Bari, Italy

X. Huang, J. Lin, Q. Ouyang, T. Wang, Y. Xie, R. Xu, S. Xue, J. Zhang, L. Zhang, W. Zhao

Institute of High Energy Physics, Academia Sinica, Beijing, The People's Republic of China⁸

D. Abbaneo, G. Boix,⁶ O. Buchmüller, M. Cattaneo, F. Cerutti, V. Ciulli, G. Davies, G. Dissertori, H. Drevermann, R.W. Forty, M. Frank, F. Gianotti, T.C. Greening, A.W. Halley, J.B. Hansen, J. Harvey, P. Janot, B. Jost, M. Kado, O. Leroy, P. Maley, P. Mato, A. Minten, A. Moutoussi, F. Ranjard, L. Rolandi, D. Schlatter, M. Schmitt,²⁰ O. Schneider,² P. Spagnolo, W. Tejessy, F. Teubert, E. Tournefier, A. Valassi, A.E. Wright

European Laboratory for Particle Physics (CERN), CH-1211 Geneva 23, Switzerland

Z. Ajaltouni, F. Badaud, G. Chazelle, O. Deschamps, S. Dessagne, A. Falvard, C. Ferdi, P. Gay, C. Guicheney, P. Henrard, J. Jousset, B. Michel, S. Monteil, J-C. Montret, D. Pallin, J.M. Pascolo, P. Perret, F. Podlyski

Laboratoire de Physique Corpusculaire, Université Blaise Pascal, IN²P³-CNRS, Clermont-Ferrand, F-63177 Aubière, France

J.D. Hansen, J.R. Hansen, P.H. Hansen,¹ B.S. Nilsson, B. Rensch, A. Wäänänen

Niels Bohr Institute, 2100 Copenhagen, DK-Denmark⁹

G. Daskalakis, A. Kyriakis, C. Markou, E. Simopoulou, A. Vayaki

Nuclear Research Center Demokritos (NRCD), GR-15310 Attiki, Greece

A. Blondel, J.-C. Brient, F. Machefert, A. Rougé, M. Swynghedauw, R. Tanaka, H. Videau

Laboratoire de Physique Nucléaire et des Hautes Energies, Ecole Polytechnique, IN²P³-CNRS, F-91128 Palaiseau Cedex, France

E. Focardi, G. Parrini, K. Zachariadou

Dipartimento di Fisica, Università di Firenze, INFN Sezione di Firenze, I-50125 Firenze, Italy

M. Corden, C. Georgiopoulos

Supercomputer Computations Research Institute, Florida State University, Tallahassee, FL 32306-4052, USA^{13,14}

A. Antonelli, G. Bencivenni, G. Bologna,⁴ F. Bossi, P. Campana, G. Capon, V. Chiarella, P. Laurelli, G. Mannonchi,^{1,5} F. Murtas, G.P. Murtas, L. Passalacqua, M. Pepe-Altarelli

Laboratori Nazionali dell'INFN (LNF-INFN), I-00044 Frascati, Italy

M. Chalmers, J. Kennedy, J.G. Lynch, P. Negus, V. O'Shea, B. Raeven, D. Smith, P. Teixeira-Dias, A.S. Thompson, J.J. Ward

*Department of Physics and Astronomy, University of Glasgow, Glasgow G12 8QQ, United Kingdom*¹⁰
R. Cavanaugh, S. Dhamotharan, C. Geweniger,¹ P. Hanke, V. Hepp, E.E. Kluge, G. Leibenguth, A. Putzer, K. Tittel, S. Werner,¹⁹ M. Wunsch¹⁹

*Kirchhoff-Institut für Physik, Universität Heidelberg, D-69120 Heidelberg, Germany*¹⁶

R. Beuselinck, D.M. Binnie, W. Cameron, P.J. Dornan, M. Girone, S. Goodsir, N. Marinelli, E.B. Martin, J. Nash, J. Nowell, H. Przysieszniak,¹ A. Sciabà, J.K. Sedgbeer, J.C. Thompson,²⁴ E. Thomson, M.D. Williams

*Department of Physics, Imperial College, London SW7 2BZ, United Kingdom*¹⁰

V.M. Ghete, P. Girtler, E. Kneringer, D. Kuhn, G. Rudolph

*Institut für Experimentalphysik, Universität Innsbruck, A-6020 Innsbruck, Austria*¹⁸

C.K. Bowdery, P.G. Buck, G. Ellis, A.J. Finch, F. Foster, G. Hughes, R.W.L. Jones, N.A. Robertson, M. Smizanska, M.I. Williams

*Department of Physics, University of Lancaster, Lancaster LA1 4YB, United Kingdom*¹⁰

I. Giehl, F. Hölldorfer, K. Jakobs, K. Kleinknecht, M. Kröcker, A.-S. Müller, H.-A. Nürnbergger, G. Quast, B. Renk, E. Rohne, H.-G. Sander, S. Schmeling, H. Wachsmuth C. Zeitnitz, T. Ziegler

*Institut für Physik, Universität Mainz, D-55099 Mainz, Germany*¹⁶

A. Bonissent, J. Carr, P. Coyle, A. Ealet, D. Fouchez, A. Tilquin

Centre de Physique des Particules, Faculté des Sciences de Luminy, IN²P³-CNRS, F-13288 Marseille, France

M. Aleppo, M. Antonelli, S. Gilardoni, F. Ragusa

Dipartimento di Fisica, Università di Milano e INFN Sezione di Milano, I-20133 Milano, Italy.

V. Büscher, H. Dietl, G. Ganis, K. Hüttmann, G. Lütjens, C. Mannert, W. Männer, H.-G. Moser, S. Schael, R. Settles, H. Seywerd, H. Stenzel, W. Wiedenmann, G. Wolf

*Max-Planck-Institut für Physik, Werner-Heisenberg-Institut, D-80805 München, Germany*¹⁶

P. Azzurri, J. Boucrot, O. Callot, S. Chen, M. Davier, L. Duflot, J.-F. Grivaz, Ph. Heusse, A. Jacholkowska,¹ J. Lefrançois, L. Serin, J.-J. Veillet, I. Videau,¹ J.-B. de Vivie de Régie, D. Zerwas

Laboratoire de l'Accélérateur Linéaire, Université de Paris-Sud, IN²P³-CNRS, F-91898 Orsay Cedex, France

G. Bagliesi, T. Boccali, C. Bozzi,¹² G. Calderini, R. Dell'Orso, I. Ferrante, A. Giassi, A. Gregorio, F. Ligabue, P.S. Marrocchesi, A. Messineo, F. Palla, G. Rizzo, G. Sanguinetti, G. Sguazzoni, R. Tenchini,¹ A. Venturi, P.G. Verdini

Dipartimento di Fisica dell'Università, INFN Sezione di Pisa, e Scuola Normale Superiore, I-56010 Pisa, Italy

G.A. Blair, J. Coles, G. Cowan, M.G. Green, D.E. Hutchcroft, L.T. Jones, T. Medcalf, J.A. Strong

*Department of Physics, Royal Holloway & Bedford New College, University of London, Surrey TW20 OEX, United Kingdom*¹⁰

D.R. Botterill, R.W. Clift, T.R. Edgecock, P.R. Norton, I.R. Tomalin

*Particle Physics Dept., Rutherford Appleton Laboratory, Chilton, Didcot, Oxon OX11 0QX, United Kingdom*¹⁰

B. Bloch-Devaux, P. Colas, B. Fabbro, G. Faïf, E. Lançon, M.-C. Lemaire, E. Locci, P. Perez, J. Rander, J.-F. Renardy, A. Rosowsky, P. Seager,²³ A. Trabelsi,²¹ B. Tuchming, B. Vallage

CEA, DAPNIA/Service de Physique des Particules, CE-Saclay, F-91191 Gif-sur-Yvette Cedex, France¹⁷

S.N. Black, J.H. Dann, C. Loomis, H.Y. Kim, N. Konstantinidis, A.M. Litke, M.A. McNeil, G. Taylor

Institute for Particle Physics, University of California at Santa Cruz, Santa Cruz, CA 95064, USA²²

C.N. Booth, S. Cartwright, F. Combley, P.N. Hodgson, M. Lehto, L.F. Thompson

Department of Physics, University of Sheffield, Sheffield S3 7RH, United Kingdom¹⁰

K. Affholderbach, A. Böhrer, S. Brandt, C. Grupen, J. Hess, A. Misiejuk, G. Prange, U. Sieler

Fachbereich Physik, Universität Siegen, D-57068 Siegen, Germany¹⁶

C. Borean, G. Giannini, B. Gobbo

Dipartimento di Fisica, Università di Trieste e INFN Sezione di Trieste, I-34127 Trieste, Italy

J. Putz, J. Rothberg, S. Wasserbaech, R.W. Williams

Experimental Elementary Particle Physics, University of Washington, WA 98195 Seattle, U.S.A.

S.R. Armstrong, P. Elmer, D.P.S. Ferguson, Y. Gao, S. González, O.J. Hayes, H. Hu, S. Jin, J. Kile, P.A. McNamara III, J. Nielsen, W. Orejudos, Y.B. Pan, Y. Saadi, I.J. Scott, J. Walsh, J.H. von Wimmersperg-Toeller, Sau Lan Wu, X. Wu, G. Zobernig

Department of Physics, University of Wisconsin, Madison, WI 53706, USA¹¹

¹Also at CERN, 1211 Geneva 23, Switzerland.

²Now at Université de Lausanne, 1015 Lausanne, Switzerland.

³Also at Centro Siciliano di Fisica Nucleare e Struttura della Materia, INFN Sezione di Catania, 95129 Catania, Italy.

⁴Also Istituto di Fisica Generale, Università di Torino, 10125 Torino, Italy.

⁵Also Istituto di Cosmo-Geofisica del C.N.R., Torino, Italy.

⁶Supported by the Commission of the European Communities, contract ERBFMBICT982894.

⁷Supported by CICYT, Spain.

⁸Supported by the National Science Foundation of China.

⁹Supported by the Danish Natural Science Research Council.

¹⁰Supported by the UK Particle Physics and Astronomy Research Council.

¹¹Supported by the US Department of Energy, grant DE-FG0295-ER40896.

¹²Now at INFN Sezione di Ferrara, 44100 Ferrara, Italy.

¹³Supported by the US Department of Energy, contract DE-FG05-92ER40742.

¹⁴Supported by the US Department of Energy, contract DE-FC05-85ER250000.

¹⁵Permanent address: Universitat de Barcelona, 08208 Barcelona, Spain.

¹⁶Supported by the Bundesministerium für Bildung, Wissenschaft, Forschung und Technologie, Germany.

¹⁷Supported by the Direction des Sciences de la Matière, C.E.A.

¹⁸Supported by the Austrian Ministry for Science and Transport.

¹⁹Now at SAP AG, 69185 Walldorf, Germany

²⁰Now at Harvard University, Cambridge, MA 02138, U.S.A.

²¹Now at Département de Physique, Faculté des Sciences de Tunis, 1060 Le Belvédère, Tunisia.

²²Supported by the US Department of Energy, grant DE-FG03-92ER40689.

²³Supported by the Commission of the European Communities, contract ERBFMBICT982874.

²⁴Also at Rutherford Appleton Laboratory, Chilton, Didcot, UK.

1 Introduction

The existence of Bose-Einstein correlations between identical bosons in reactions leading to hadronic final states is well established. This effect leads to an enhancement of the two-particle differential cross section for pairs of identical pions close in phase space, which was first observed experimentally in $p\bar{p}$ collisions [1]. Bose-Einstein correlations were also studied in hadronic Z decays [2, 3, 4], and observations of these correlations in W -pair production at LEP 2 have already been reported [5–9]. Theoretically, it is unclear to what extent Bose-Einstein interference occurs between the decay products of the two W 's in the $WW \rightarrow q\bar{q}q\bar{q}$ channel [10]. Such interference, if sizeable, may influence the W mass measurement [11]. In this analysis further studies of these correlations in W -pair production in e^+e^- annihilations at LEP 2 are reported, based on the data collected by ALEPH in 1996, 1997 and 1998.

The principle of the analysis is as follows: Bose-Einstein correlations are first analysed from a high statistics Z decay sample. The Bose-Einstein correlations for $udsc$ quarks present in W decays are extracted from the natural mixture of $udscb$ flavours in Z decays by means of b tagging. The distribution of Bose-Einstein correlations in these $udsc$ flavours is well reproduced by a tuned version of a model of Lönnblad and Sjöstrand [12] implemented in JETSET. This Monte Carlo is used to predict the expected effect in W decays; its role is mainly to account for the different kinematics, background and selection biases in the W sample with respect to the Z decays. This Monte Carlo prediction is compared with the measurement of the Bose-Einstein correlations in $WW \rightarrow q\bar{q}\ell\nu$ events and also in $WW \rightarrow q\bar{q}q\bar{q}$ under the assumption that the two W 's decay independently. These comparisons are independent of the modeling of the Bose-Einstein correlations in the Monte Carlo which is only used to propagate the observed effect in $udsc$ flavours at the Z peak to the W -pair events. Finally a variant of model [12] allowing Bose-Einstein correlations among different W 's is tested by comparison with the $WW \rightarrow q\bar{q}q\bar{q}$ distribution.

2 The ALEPH detector

The ALEPH detector is described in detail elsewhere [13, 14]. The most important component for this analysis is the tracking system. Starting from the interaction point, one first encounters the silicon strip vertex detector (VDET) [15]. The VDET has two layers each providing measurements of the $r\phi$ and z coordinates, with a resolution of $10\ \mu\text{m}$ in $r\phi$ and $15\ \mu\text{m}$ in z . The VDET lies within a small cylindrical drift chamber (ITC), which measures up to eight $r\phi$ coordinates per track. The ITC is in turn enclosed within a large time projection chamber (TPC), lying between radii of 31 and 180 cm. The TPC provides up to 21 three-dimensional coordinates per track. Its resolution is about $200\ \mu\text{m}$ in $r\phi$ and 1 mm in z . It also provides dE/dx information, with a resolution of up to 4.4%, for particle identification. A momentum resolution of $\sigma(P_T)/P_T = 6 \times 10^{-4}P_T \oplus 0.005$ (with the transverse momentum P_T expressed in GeV/c) is achieved. The tracking efficiency in the TPC is close to 100% for tracks with transverse momentum above 200 MeV/c and falls sharply below this value.

Outside the TPC there is an electromagnetic calorimeter (ECAL), a sandwich of lead sheets and proportional tubes. Highly granular transverse and longitudinal measurements of electromagnetic showers are provided by projective towers, which are segmented longitudinally in three storeys. The achieved energy resolution is $\sigma(E)/E = 0.18/\sqrt{E} + 0.009$ (E in GeV). These subdetectors are surrounded by a superconducting solenoid producing a 1.5 T magnetic field. A hadron calorimeter (HCAL) surrounds the solenoid and is used for hadron energy measurement as well as for muon identification. Muons are also measured outside the calorimeter in two double layers of limited-streamer tubes. The information from the tracking detectors and the calorimeters is combined by an energy flow algorithm [14], which provides for each event a list of energy flow objects (charged and neutral hadrons, photons, muons and electrons).

3 Data samples and event selection

In this analysis, Z data recorded in 1997 corresponding to an integrated luminosity \mathcal{L} of 2.3 pb^{-1} are used to tune the different Monte Carlo models of Bose-Einstein correlations. These data are taken with the same detector configuration as the W^+W^- events. The measurement of Bose-Einstein correlations in W^+W^- events uses the data recorded at 172.1 GeV ($\mathcal{L} = 10.7 \text{ pb}^{-1}$), 182.6 GeV ($\mathcal{L} = 56.8 \text{ pb}^{-1}$) and 188.6 GeV ($\mathcal{L} = 174.2 \text{ pb}^{-1}$).

Hadronic Z decays. The offline selection of the hadronic events is based on tracks that pass through a cylinder of 2 cm radius and 10 cm half length centered at the interaction point. The tracks are also required to have at least four hits in the TPC and polar angle in the range $|\cos \theta| < 0.95$. Events are accepted if they have at least five of these tracks and if their total energy exceeds 10% of the centre of mass energy.

Fully hadronic W pair decays. The track selection described above is also applied as a first step of the W-pair event selection. The fully hadronic W-pair decays are then selected with a neural network method [16, 17]. The output of the neural network is peaked at 1 for signal and -1 for $q\bar{q}$ background. In this analysis, events with a neural network output greater than -0.3 are retained. The background is dominated by $q\bar{q}$ events.

Semileptonic W pair decays. The $WW \rightarrow q\bar{q}e\nu_e$ and $WW \rightarrow q\bar{q}\mu\nu_\mu$ events are characterised by two well separated hadronic jets, a high-momentum lepton and missing momentum due to the undetected neutrino. Cuts based on this expected topology are applied to reject background [18]. The residual background is mainly from $WW \rightarrow q\bar{q}\tau\nu_\tau$ and $q\bar{q}$ events. A $WW \rightarrow q\bar{q}\tau\nu_\tau$ event is selected [19, 20] if it passes a series of preselection cuts and if it satisfies either a topological or a global selection. For the measurement of Bose-Einstein correlations, in contrast to the analysis used to measure the WW cross-section, a τ jet is always explicitly searched for as this allows to remove the pions from the τ decays from the hadronic part of the event. The main background comes from $WW \rightarrow q\bar{q}e\nu_e$ and $WW \rightarrow q\bar{q}\mu\nu_\mu$ events with additional contributions from $q\bar{q}$, $W\nu$ and ZZ events.

The efficiencies, purities and numbers of selected events at different centre of mass energies are reported in Table 1.

Table 1: Efficiencies, purities and numbers of selected W-pair events at different centre-of-mass energies.

Energy (GeV)	Efficiency (%)	Purity (%)	Number of selected events
WW \rightarrow qq $\bar{q}\bar{q}$ selection			
172	85.0	80.1	69
183	89.8	79.4	503
189	91.3	77.2	1449
WW \rightarrow qq $\bar{\ell}\nu$ selection			
172	79.7	95.0	44
183	80.5	94.4	330
189	78.0	95.2	1005

4 Analysis method

4.1 Fitting the Bose-Einstein correlation parameters

Bose-Einstein correlations occur for pions of the same charge. In order to detect an enhancement of the two-particle cross section for pairs of identical pions, a sample identical in all aspects with the like-charged pion pair sample, except for Bose-Einstein correlations, is needed as reference. In this paper, the unlike-charged pion pairs are taken as the reference sample in order to minimize systematic experimental errors related to track reconstruction and acceptance. The ratio of the number of like-charged pairs ($N^{++,--}$) to the number of unlike-charged pairs (N^{+-}) is measured as a function of Q given by $\sqrt{(\mathbf{p}_1 - \mathbf{p}_2)^2 - (E_1 - E_2)^2}$ where $\mathbf{p}_1 - \mathbf{p}_2$ and $E_1 - E_2$ are the differences in 3-momentum and energy of the two particles. Since the unlike-charged pion pairs are not free from other sources of correlations, the ratio for the data is corrected by dividing by the same ratio obtained from the Monte Carlo without Bose-Einstein correlations (“standard Monte Carlo”). In this way corrections for resonance decays and for acceptance effects are taken into account. This new ratio is called $R^*(Q)$ in the following, with:

$$R^*(Q) = \left(\frac{N_{\pi^{++},--}(Q)}{N_{\pi^{+-}}(Q)} \right)^{\text{data}} \bigg/ \left(\frac{N_{\pi^{++},--}(Q)}{N_{\pi^{+-}}(Q)} \right)_{\text{no BE}}^{\text{MC}}. \quad (1)$$

The Bose-Einstein enhancement occurs at low values of Q , and is parameterised throughout this paper by the widely used formula

$$R^*(Q) = \kappa(1 + \epsilon Q)(1 + \lambda e^{-\sigma^2 Q^2}), \quad (2)$$

where κ is the normalization factor and the term $1 + \epsilon Q$ takes into account some long-range correlations, due to charge conservation or energy-momentum conservation. The $1 + \lambda e^{-\sigma^2 Q^2}$ factor describes the Bose-Einstein effect. The parameter λ gives the effective strength of the Bose-Einstein correlations while the parameter σ is related to the source size.

Theoretically it is unclear whether Bose-Einstein correlations between pions from different W 's should have the same source size as the ones from the same W [21]. Two fits are therefore performed in this analysis using the parameterisation of Eq. (2). In the first, four parameters are fitted: κ , ϵ , λ and σ in the Q range between 0 and 3 GeV. The λ and σ parameter values are used to calculate an integral of the Bose-Einstein signal $\int_0^\infty \lambda e^{-\sigma^2 Q^2} dQ = \frac{\sqrt{\pi}}{2} \frac{\lambda}{\sigma}$ which is compared in data and Monte Carlo. In the second, only λ is fitted in the Q range between 0 and 0.4 GeV, and is compared in data and Monte Carlo.

4.2 Pion selection

The pion selection rejects tracks identified by the energy flow algorithm as electrons or muons or originating from V^0 decay. Pairs of electrons from γ conversion give a peak near $Q^2 = 0$ in the unlike-charged pion pair distribution. Two tracks are identified as a conversion if their distance of minimum approach is less than 1 cm in the $r\phi$ projection, less than 2 cm in z , their invariant mass less than 30 MeV/ c^2 and their measured dE/dx within 3σ of that expected for electrons. In addition, tracks with momentum smaller than 5 GeV/ c and not associated with conversions are rejected if their measured dE/dx is within 3σ of that expected for an electron.

Successive arcs of spiraling tracks passing near the TPC membrane at $z = 0$ are sometimes split into multiple tracks, which are very close in momentum space. To reject them, tracks produced with a polar angle in the range $[87.5^\circ, 92.5^\circ]$ are required to have at least three hits in the five first pad layers of the TPC.

All other charged particles are treated as pions. Monte Carlo studies show that the purity of the $\pi\pi$ pairs is about 80% in the low Q region where Bose-Einstein correlations are expected to take place.

4.3 Monte Carlo

Hadronic Z decays are simulated at a centre-of-mass energy of 91 GeV with the PYTHIA [22] generator. These events are used to tune the different models simulating the Bose-Einstein correlations. W -pair events are generated with KORALW [23]. The $q\bar{q}$ and ZZ backgrounds are produced with PYTHIA. In all cases, the hadronisation scheme used is JETSET [22]. The Monte Carlo distributions shown in this paper include simulations of particle interactions in the detector and full detector response.

The Bose-Einstein correlations are simulated with a JETSET routine ([12], model BE₃). The default parameters of this model are changed to $\lambda_{\text{JETSET}}^{\text{input}} = 2.3$ and $R_{\text{JETSET}}^{\text{input}} = 0.26$ GeV after tuning to Z data. The parameter $\lambda_{\text{JETSET}}^{\text{input}}$ controls the strength of the Bose-Einstein correlations while the parameter $R_{\text{JETSET}}^{\text{input}}$ controls the source size. Residual discrepancies between data and Monte Carlo are corrected for as described later. This Monte Carlo is the basic tool to compare data to predictions in W -pair decays.

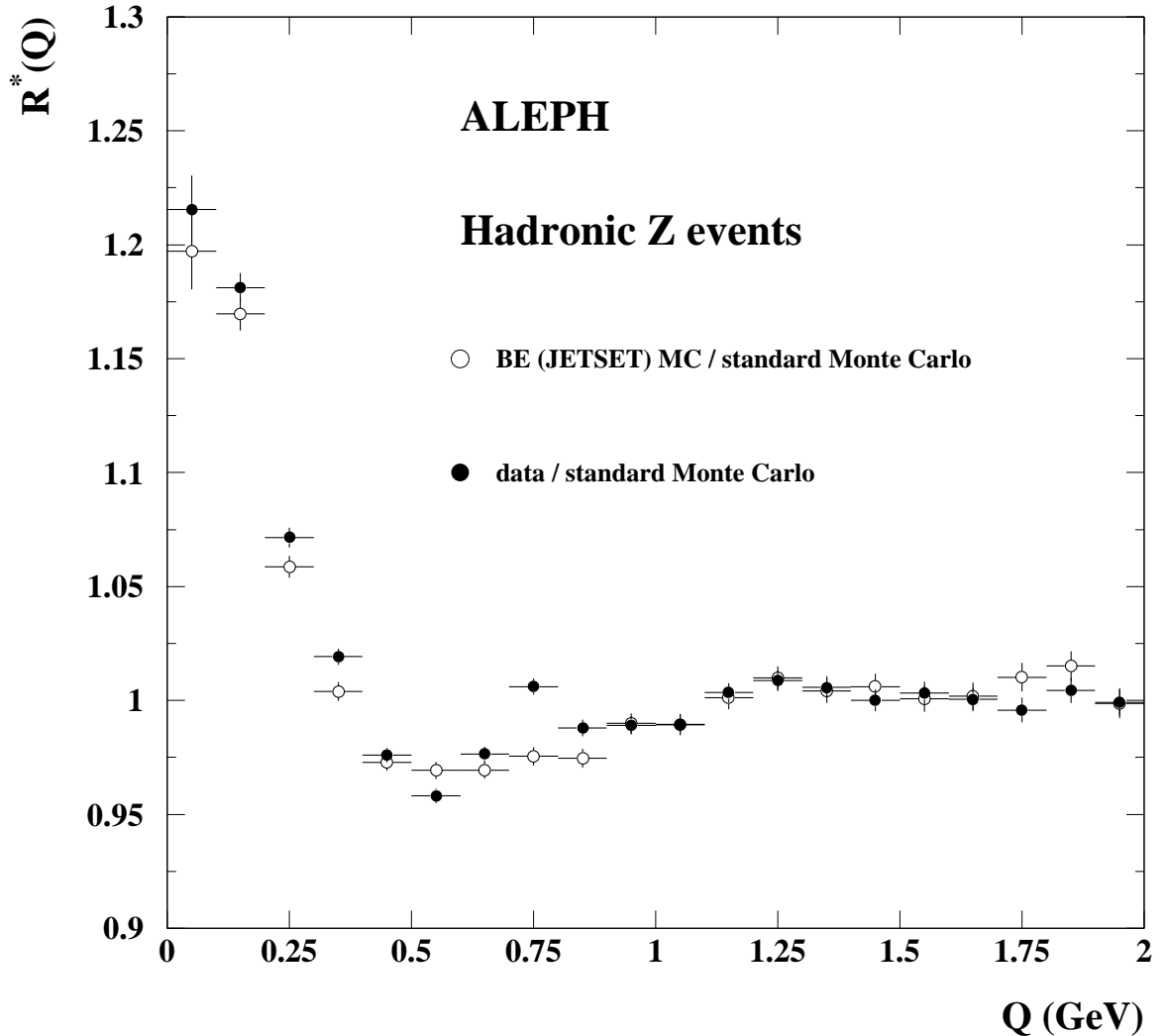


Figure 1: Comparison of $R^*(Q)$ for the hadronic Z decay data and the JETSET Monte Carlo model of the Bose-Einstein effect. Only statistical errors are shown.

Other models were tried that describe Bose-Einstein correlations by introducing event weights based on the Q -values between the pions [24, 25]. Since these models could not be tuned to Z data with reasonable values of weights [18], they were not used for the analysis of W data.

4.4 Bose-Einstein correlations at the Z and Monte Carlo tuning

Figure 1 shows the ratio $R^*(Q)$ defined in Eq. (1) for the Z data compared with the JETSET Bose-Einstein model.

The values of the fitted parameters are given in Table 2 for JETSET and the data. The observed difference comes mainly from the $Z \rightarrow b\bar{b}$ decays as shown in Fig. 2 and described below.

ALEPH

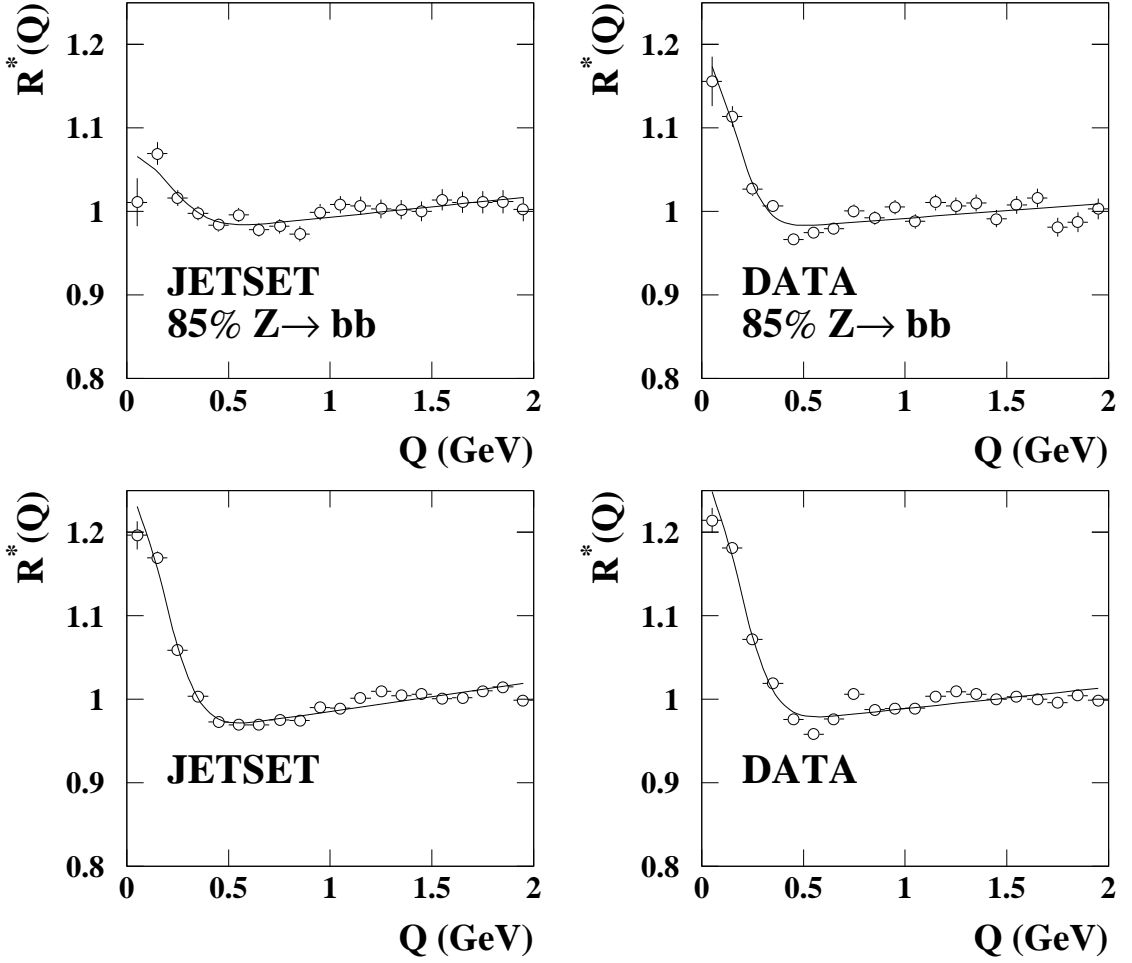


Figure 2: $R^*(Q)$ with (top) and without (bottom) a $b\bar{b}$ tag for data (right) and Monte Carlo JETSET (left). The solid curves show the results of the fits based on the parameterisation of Eq. (2). Only statistical errors are shown.

Table 2: Fitted parameters obtained at $\sqrt{s} = 91$ GeV for the data and for the JETSET Monte Carlo model. The quantity $C_{\lambda\sigma}$ is the correlation coefficient between the errors on λ and σ . Only statistical errors are shown.

	κ	ϵ (GeV ⁻¹)	λ	σ (GeV ⁻¹)	$C_{\lambda\sigma}$
JETSET	0.966 ± 0.002	0.019 ± 0.002	0.29 ± 0.01	4.31 ± 0.11	0.59
data	0.977 ± 0.002	0.010 ± 0.001	0.30 ± 0.01	4.27 ± 0.09	0.57
data udsc	0.978 ± 0.002	0.010 ± 0.001	0.35 ± 0.01	4.29 ± 0.08	0.58
One-parameter fit					
JETSET			0.264 ± 0.008		
data	0.978	0.0097	0.294 ± 0.007	4.242	
data udsc			0.343 ± 0.007		

The effect of Bose-Einstein correlations is expected to be different in events containing b quarks and events containing udsc quarks. As an example, if one pion comes from fragmentation and another one from the decay of a B meson, no detectable Bose-Einstein effect is expected in the pair. As W bosons do not decay into b quarks, the Bose-Einstein correlations are studied for events without b quarks. Fits of the Bose-Einstein enhancement are performed for full sample and for a sample enriched in $b\bar{b}$ events [26] both in data and Monte Carlo as shown in Fig. 2. The value of λ for udsc and b flavours is extrapolated from these samples, assuming that $\lambda^{1,2} = \rho^{1,2}\lambda_b + (1 - \rho^{1,2})\lambda_{udsc}$ where $\rho^{1,2}$ are the fractions of unlike-charged pairs coming from $b\bar{b}$ events at low Q obtained from Monte Carlo without Bose-Einstein correlations, and $\lambda^{1,2}$ the fit results for the two samples. After tuning at the Z peak, the differences between data and JETSET Monte Carlo in λ_{udsc} and $\int_0^\infty \lambda e^{-\sigma^2 Q^2} dQ$ are $(0 \pm 6)\%$ and $(11 \pm 7)\%$, respectively.

Figure 3 shows the $R^*(Q)$ distributions for udsc components in data and Monte Carlo. They are obtained by extrapolating the udsc component using the fitted values of λ_b and λ_{udsc} described above. The fit results to the pure udsc data sample are given in Table 2.

Residual discrepancies between data and Monte Carlo seen in Fig. 3 are taken into account by calculating a bin by bin correction function $C(Q)$

$$C(Q) = \frac{R^*(Q)_{\text{data}}^{Z_{udsc}}}{R^*(Q)_{\text{MC}}^{Z_{udsc}}}.$$

After applying these corrections to the JETSET udsc distribution the Monte Carlo points coincide with the data points by construction and thus the central values of fit results to this distribution are identical to those of the data. The statistical errors of the tuning, 6% for λ_{udsc} and 7% for $\int_0^\infty \lambda e^{-\sigma^2 Q^2} dQ$, are taken as the systematic uncertainties on the Bose-Einstein Monte Carlo tuning at the Z.

The corrections $C(Q)$ are used to reweight the Monte Carlo distributions bin by bin in the study of Bose-Einstein correlations in W-pair decays. For comparisons between data and Monte Carlo in W-pair decays, additional systematic errors could arise for effects that are different in Z udsc and W-pair decays. The apparatus and the event reconstruction programs are however identical for Z and W-pair events. Different kinematics, background, pion purity and selection biases are accounted for by the JETSET Monte Carlo with negligible systematic errors compared to the systematic errors of the tuning at the Z.

5 Bose-Einstein correlations in W-pair decays

The analysis is performed at each centre-of-mass energy. No significant dependence of the fitted parameters on the centre-of-mass energy is observed. Like- and unlike-charged pair distributions in Q at different energies are therefore added and the ratio $R^*(Q)$ is fitted. As stated in Sec. 4.1 four- and one-parameter fits are performed. For the one-parameter fit, the values of σ , κ and ϵ are fixed to the weighted average values of the parameters fitted in W events ($WW \rightarrow q\bar{q}\ell\nu$ and $WW \rightarrow q\bar{q}q\bar{q}$) and Z events.

Semileptonic W pair decays. In the $WW \rightarrow q\bar{q}\ell\nu$ channel, Bose-Einstein correlations are studied in the $q\bar{q}$ system. They are assumed to be the same in the WW signal and

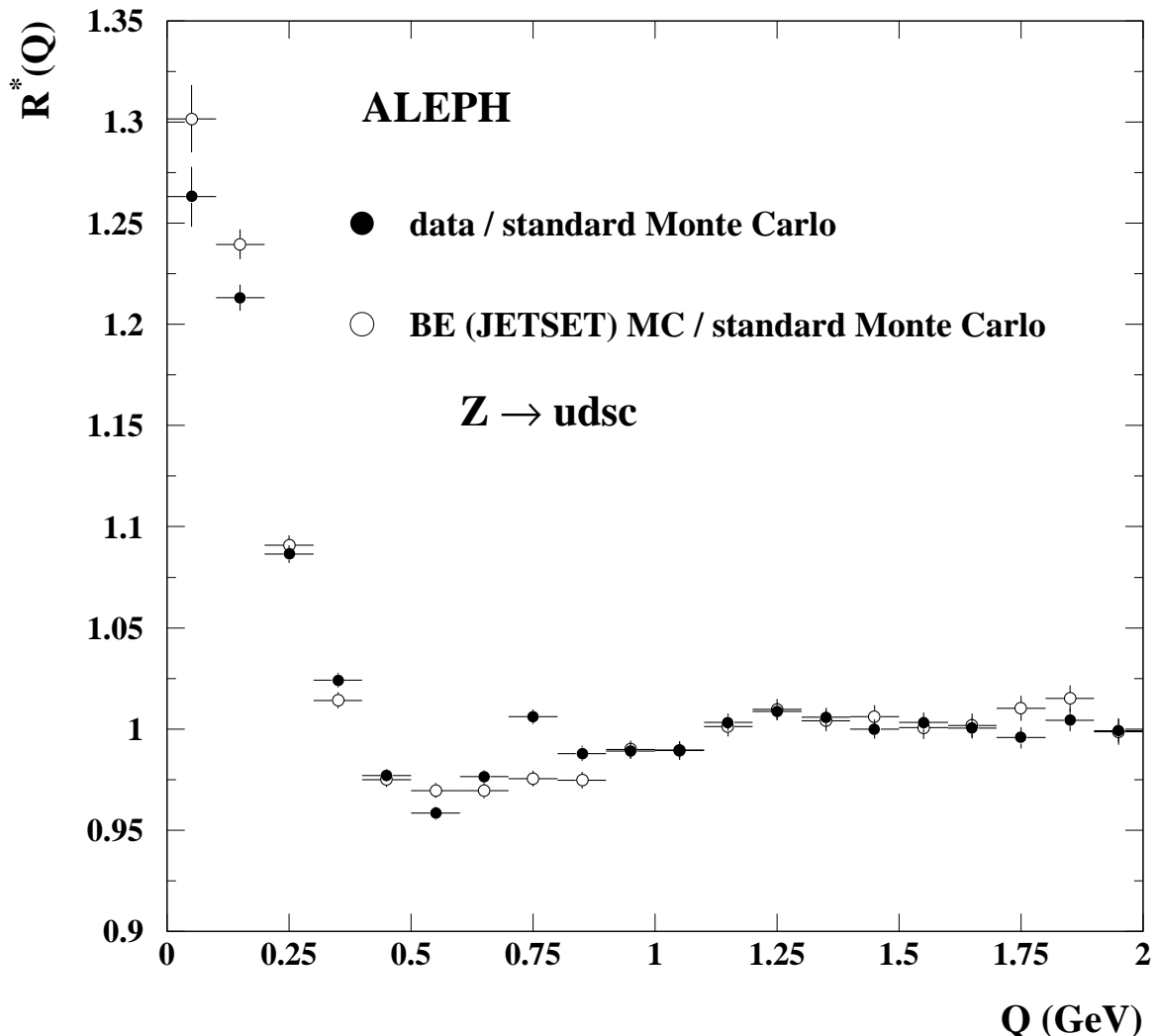


Figure 3: Comparison of $R^*(Q)$ for the hadronic Z decay data and the JETSET Monte Carlo model tuned at the Z peak, both extrapolated to a pure $udsc$ sample. Only statistical errors are shown.

in the 5% background. This small background is therefore neglected in the Monte Carlo, with and without the Bose-Einstein effect. The fit results are reported in Table 3. Figure 4 shows the comparison of the data to the JETSET Monte Carlo model tuned and corrected at the Z peak. Also shown as a solid curve is the fit result for the data.

Fully hadronic W pair decays. In this channel, the $q\bar{q}$ background is included in the Monte Carlo predictions when the comparisons with the data are made. The Bose-Einstein correlations are generated using the parameters tuned at 91 GeV as described in Section 4.4. The results obtained are not changed if the background contribution is changed by $\pm 5\%$ [18]. The fit results are reported in Table 4. In this table and in what follows, “BEI” (Bose-Einstein inside) stands for the case where there are no Bose-Einstein correlations between decay products of different W’s, and “BEB” (Bose-Einstein both) for the case where there are. Figure 5 shows the comparison of the data to both models and the result

Table 3: Fitted parameters in the $WW \rightarrow q\bar{q}\ell\nu$ channel for data and JETSET Monte Carlo. The quantity $C_{\lambda\sigma}$ is the correlation coefficient between the errors on λ and σ . The first error is the statistical fit error and the second is the JETSET systematic error on λ and $\int_0^\infty \lambda e^{-\sigma^2 Q^2} dQ$.

	κ	ϵ (GeV^{-1})	λ	σ (GeV^{-1})	$C_{\lambda\sigma}$	$\int_0^\infty \lambda e^{-\sigma^2 Q^2} dQ$
JETSET	0.967 ± 0.004	0.019 ± 0.003	0.30 ± 0.02	4.04 ± 0.14	0.53	$0.066 \pm 0.003 \pm 0.005$
data	0.995 ± 0.010	0.000 ± 0.010	0.23 ± 0.06	3.89 ± 0.55	0.46	0.053 ± 0.011
One-parameter fit						
JETSET	0.978	0.0097	$0.30 \pm 0.01 \pm 0.02$	4.242		
data			0.29 ± 0.05			

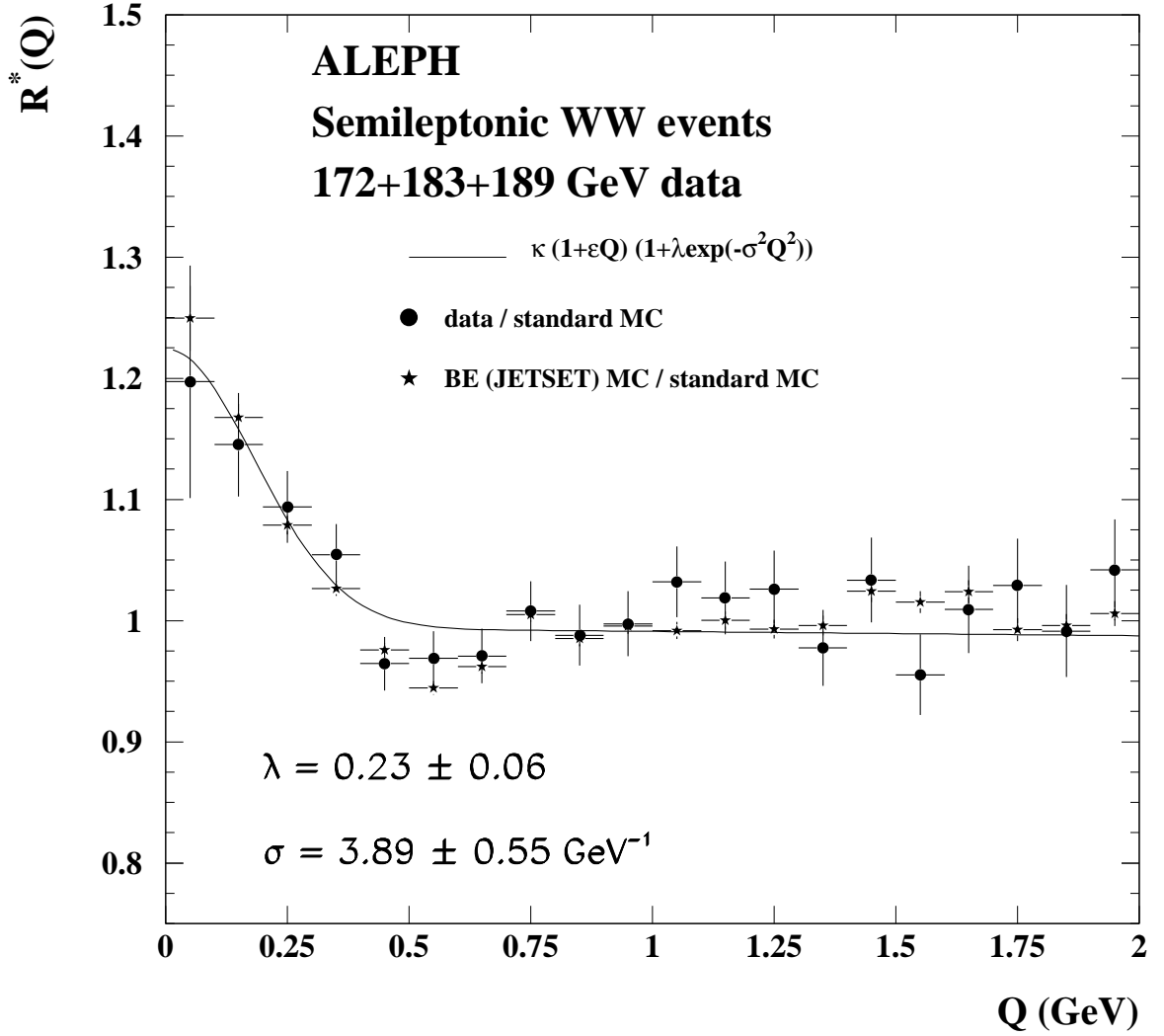


Figure 4: $R^*(Q)$ for data and Monte Carlo with Bose-Einstein correlations for semileptonic WW events. Only statistical errors are shown. The systematic errors on the Monte Carlo predictions are given in Table 5. The solid curve shows the result of the fit to the data.

of the fit to the data.

Table 4: Fitted parameters in the $WW \rightarrow q\bar{q}q\bar{q}$ channel for data and two JETSET models BEB and BEI. The quantity $C_{\lambda\sigma}$ is the correlation coefficient between the errors on λ and σ . The first error is the statistical fit error and the second is the JETSET systematic error on λ and $\int_0^\infty \lambda e^{-\sigma^2 Q^2} dQ$.

	κ	ϵ (GeV $^{-1}$)	λ	σ (GeV $^{-1}$)	$C_{\lambda\sigma}$	$\int_0^\infty \lambda e^{-\sigma^2 Q^2} dQ$
BEB	0.980 ± 0.002	0.008 ± 0.001	0.35 ± 0.01	4.45 ± 0.11	0.64	$0.069 \pm 0.002 \pm 0.005$
BEI	0.989 ± 0.002	0.003 ± 0.001	0.27 ± 0.02	4.66 ± 0.16	0.65	$0.051 \pm 0.002 \pm 0.004$
data	0.987 ± 0.007	0.007 ± 0.004	0.23 ± 0.03	4.26 ± 0.43	0.61	0.47 ± 0.006
One-parameter fit						
BEB			$0.33 \pm 0.01 \pm 0.02$			
BEI	0.978	0.0097	$0.27 \pm 0.01 \pm 0.02$	4.242		
data			0.25 ± 0.02			

Bin-to-bin correlations are important in the Q distribution because in each event every pion enters through several combinations. These correlations could lead to an increase of the statistical uncertainties on the fit parameters [8, 27]. These correlations have been measured in the data. Large bin-to-bin correlations are observed for the like- and unlike-charged sign pairs. They are, however, negligible for the ratio of like- to unlike-charged sign pairs; this is presumably due to the fact that the same pions contribute to the two distributions and to their bin-to-bin correlations. Indeed, four- and one-parameter fits performed for 225 Monte Carlo experiments with the same statistics as the data confirm that the fit errors are correct. The ratio of the Gaussian width of the λ and $\int_0^\infty \lambda e^{-\sigma^2 Q^2} dQ$ distributions for the results of these experiments to the average fit errors are 0.92 ± 0.05 and 1.04 ± 0.07 , respectively.

Table 5: Results for the data and the JETSET Monte Carlo, tuned and corrected at the Z peak, for the one-parameter fit and for $\int_0^\infty \lambda e^{-\sigma^2 Q^2} dQ$. Also shown is the difference between the fully hadronic (4j) and the semileptonic (2j) decay channel, and between data and Monte Carlo in the various cases. The first error is the statistical fit error, the second corresponds to $\pm 6\%$ and $\pm 7\%$ systematic errors related to JETSET on λ and $\int_0^\infty \lambda e^{-\sigma^2 Q^2} dQ$, respectively.

Sample		λ	$\int_0^\infty \lambda e^{-\sigma^2 Q^2} dQ$
WW (4j)	JETSET (BEB)	$0.334 \pm 0.009 \pm 0.020$	$0.0689 \pm 0.0021 \pm 0.0048$
	JETSET (BEI)	$0.265 \pm 0.009 \pm 0.016$	$0.0512 \pm 0.0022 \pm 0.0036$
	data	0.246 ± 0.024	0.0472 ± 0.0058
WW (2j)	JETSET	$0.300 \pm 0.012 \pm 0.018$	$0.0662 \pm 0.0032 \pm 0.0046$
	data	0.292 ± 0.046	0.0526 ± 0.0114
Z udsc	data/JETSET	0.343 ± 0.007	0.0713 ± 0.0017
differences			
(4j data)–(2j data)		-0.046 ± 0.052	-0.0054 ± 0.0128
(4j data)–(4j JETSET (BEB))		$-0.088 \pm 0.026 \pm 0.020$	$-0.0217 \pm 0.0062 \pm 0.0048$
(4j data)–(4j JETSET (BEI))		$-0.019 \pm 0.026 \pm 0.016$	$-0.0040 \pm 0.0062 \pm 0.0036$
(2j data)–(2j JETSET)		$-0.008 \pm 0.048 \pm 0.018$	$-0.0136 \pm 0.0118 \pm 0.0046$

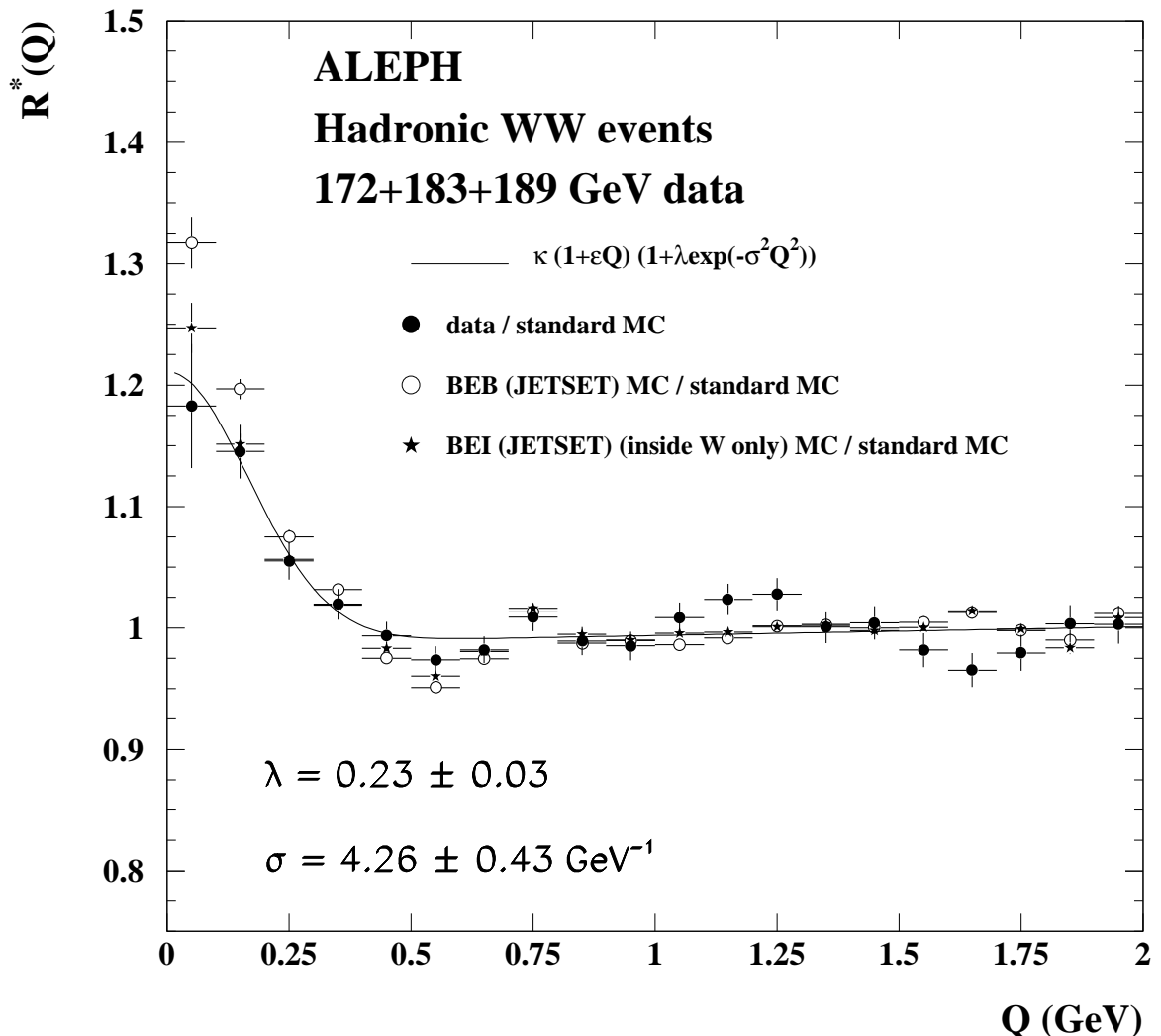


Figure 5: $R^*(Q)$ for data and Monte Carlo with Bose-Einstein correlations for hadronic WW events. Only statistical errors are shown. The systematic errors on the Monte Carlo predictions are given in Table 5. The solid curve shows the result of the fit to the data.

Statistical significance. To better quantify the agreement between data and Monte Carlo predictions the results of the one-parameter fit and also the integrated signal $\int_0^\infty \lambda e^{-\sigma^2 Q^2} dQ = \frac{\sqrt{\pi}}{2} \frac{\lambda}{\sigma}$, are reported in Table 5.

Fig. 6 and Table 5 show that the Monte Carlo is in very good agreement with the semileptonic data. Concerning fully hadronic W-pair decays there is a better agreement between data and the Monte Carlo when Bose-Einstein correlations between decay products of different W's are excluded. In both fits, their inclusion is disfavoured at the 2.7σ level.

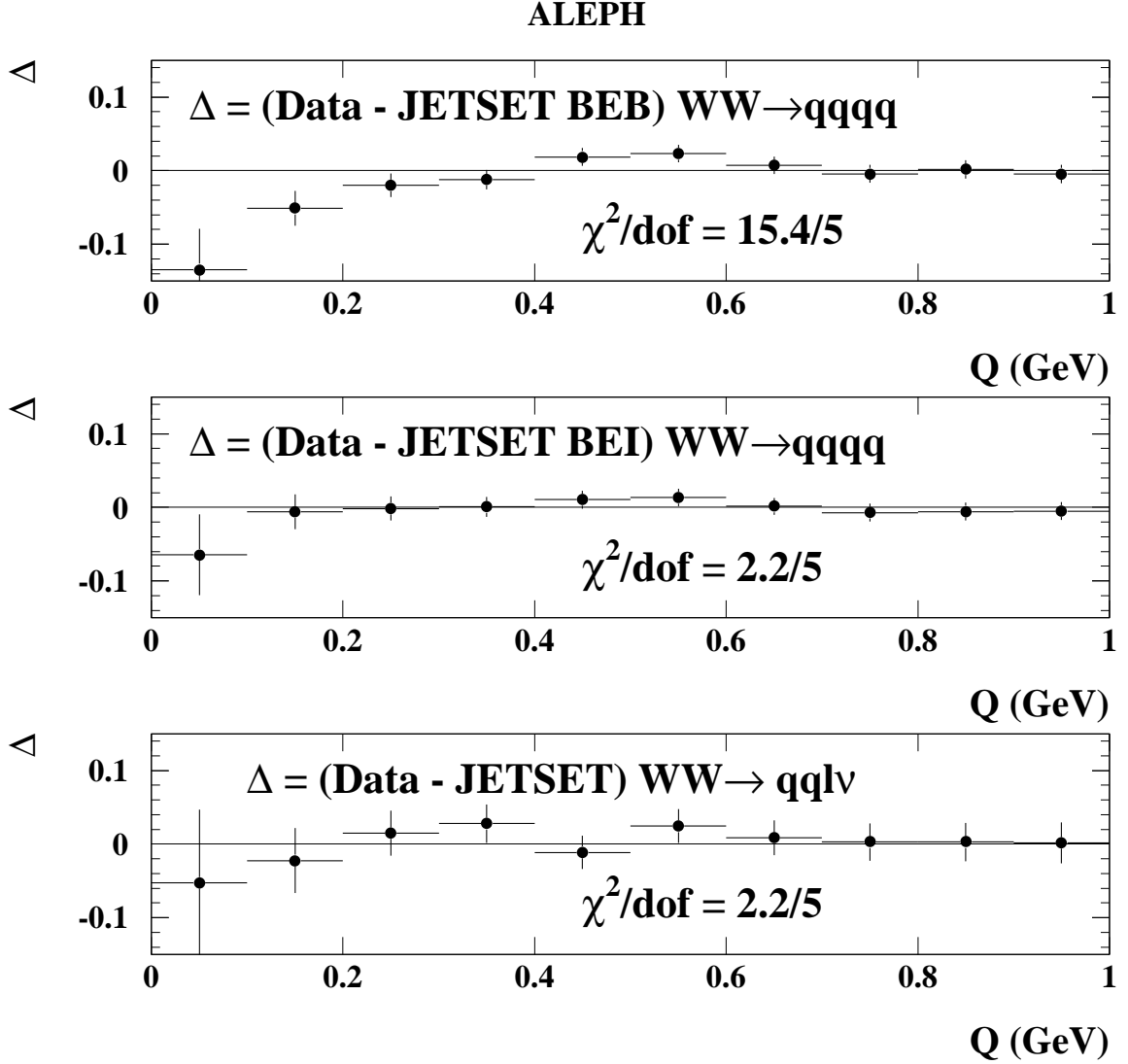


Figure 6: Differences in $R^*(Q)$ between the data and the different JETSET Monte Carlo predictions tuned and corrected at the Z peak. Only statistical errors are shown. The χ^2 is calculated for the five bins with smallest Q .

Top: difference between the data in $\text{WW} \rightarrow \text{qq}\bar{\text{q}}\bar{\text{q}}$ events and the model with Bose-Einstein correlations present between the particles produced from different W's.

Middle: difference between the data in $\text{WW} \rightarrow \text{qq}\bar{\text{q}}\bar{\text{q}}$ events and the model with Bose-Einstein correlations NOT present between the particles produced from different W's.

Bottom: difference between the data in $\text{WW} \rightarrow \text{qq}\bar{\ell}\nu$ events and the JETSET Monte Carlo model.

6 Conclusions

From the above studies the following conclusions can be drawn:

- Bose-Einstein correlations are observed in the semileptonic W-pair decays. They are well reproduced by a JETSET model tuned and corrected at the Z peak for $u\bar{d}sc$ flavours.

- In fully hadronic W-pair decays data are in better agreement with the JETSET model tuned and corrected at the Z peak where the Bose-Einstein correlations are present only for pions coming from the same W. The same JETSET model with the Bose-Einstein correlations between pions from different W's is disfavoured at the 2.7σ level.

Acknowledgment

We are indebted to our colleagues of the accelerator divisions for the outstanding performance of the LEP accelerator. Thanks are also due to the many engineering and technical personnel at CERN and at the home institutes for their contributions toward the success of ALEPH. Those of us not from member states wish to thank CERN for its hospitality.

References

- [1] G. Goldhaber et al., Phys. Rev. **120** (1960) 300.
- [2] ALEPH Collaboration, *A study of Bose-Einstein correlations in e^+e^- annihilations at 91 GeV*, Z. Phys. **C54** (1992) 75.
- [3] DELPHI Collaboration, *Bose-Einstein correlations in the hadronic decays of the Z^0* , Phys. Lett. **B286** (1992) 201.
- [4] OPAL Collaboration, *Multiplicity dependence of Bose-Einstein correlations in hadronic Z^0 decays*, Z. Phys. **C72** (1996) 389.
- [5] ALEPH Collaboration, *Bose-Einstein correlations in W-pair decays*, contribution to the XXIX International Conference on High Energy Physics, Vancouver, Canada, 23-29 July 1998, Ref. 894, ALEPH conference note ALEPH 98-065 CONF 98-035; contribution to the 1999 winter conferences, ALEPH conference note ALEPH 99-027 CONF 99-021.
- [6] DELPHI Collaboration, *Measurements of correlations between pions from different W's in $e^+e^- \rightarrow W^+W^-$ events*, Phys. Lett. **B401** (1997) 181.
- [7] OPAL Collaboration, *Bose-Einstein Correlations in $e^+e^- \rightarrow W^+W^-$ at 172 and 183 GeV*, Eur. Phys. J. **C8** (1999) 559; *Bose-Einstein Correlations in $e^+e^- \rightarrow W^+W^-$ events at 172, 183 and 189 GeV*, contribution to the Int. Europhysics Conf. on High Energy Physics 99, Tampere, Finland, 15-21 July 1999, OPAL Physics Note PN393.
- [8] DELPHI Collaboration, *Bose-Einstein Correlations Between Particles from Different W's in $e^+e^- \rightarrow W^+W^-$ Events*, DELPHI notes DELPHI 99-22 CONF 221 and DELPHI 99-159 CONF 330.
- [9] L3 Collaboration, *Study of Bose-Einstein Correlations in W-pair Production at $\sqrt{s} = 189$ GeV*, contribution to the Int. Europhysics Conf. on High Energy Physics 99, Tampere, Finland, 15-21 July 1999, L3 Note 2405.

- [10] L. Lönnblad and T. Sjöstrand, Phys. Lett. **B351** (1995) 293.
- [11] *Determination of the mass of the W boson*, in *Physics at LEP2*, CERN Report 96-01, ed. G. Altarelli, T. Sjöstrand and F. Zwirner (CERN, Geneva, 1996), Vol. 1, p. 141.
- [12] L. Lönnblad and T. Sjöstrand, Eur. Phys. J. **C2** (1998) 165.
- [13] ALEPH Collaboration, *ALEPH: a detector for electron-positron annihilations at LEP*, Nucl. Instrum. Methods **A294** (1990) 121.
- [14] ALEPH Collaboration, *Performance of the ALEPH detector at LEP*, Nucl. Instrum. Methods **A360** (1995) 481.
- [15] D. Creanza et al., *The new ALEPH Silicon Vertex Detector*, Nucl. Instrum. Methods **A409** (1998) 157.
- [16] ALEPH Collaboration, *Measurement of the W mass by direct reconstruction in e^+e^- collisions at 172 GeV*, Phys. Lett. **B422** (1998) 384.
- [17] ALEPH Collaboration, *Measurement of W-pair production in e^+e^- collisions at 183 GeV*, Phys. Lett. **B453** (1999) 107.
- [18] F. Martin, *Mesure des corrélations de Bose-Einstein dans les désintégrations de paires de Bosons W avec le détecteur ALEPH au LEP*, thesis, L.A.P.P., Université de Savoie, Chambéry (1999).
- [19] ALEPH Collaboration, *Measurement of the W-pair cross-section in e^+e^- collisions at 172 GeV*, Phys. Lett. **B415** (1997) 435.
- [20] ALEPH Collaboration, *Measurement of the W mass in e^+e^- collisions at production threshold*, Phys. Lett. **B401** (1997) 347.
- [21] K. Fialkowski and R. Wit, *Bose-Einstein effect in Monte Carlo generators*, talk presented at the XXVIII International Symposium on Multiparticle Dynamics, Delphi, 1998, to appear in the proceedings, preprint hep-ph/9810492.
- [22] T. Sjöstrand, Comp. Phys. Comm. **67** (1994) 74.
- [23] M. Skrzypek, S. Jadach, W. Placzek and Z. Wąs, Comp. Phys. Comm. **94** (1996) 216.
- [24] S. Jadach and K. Zalewski, Acta Phys. Polonica, **B28** (1997) 1363.
- [25] K. Fialkowski and R. Wit, Acta Phys. Polon. **B28** (1997) 2039; preprint TPJU-3-97, hep-ph/9703227.
- [26] ALEPH Collaboration, *A precise measurement of $\Gamma_{Z \rightarrow b\bar{b}}/\Gamma_{Z \rightarrow \text{hadrons}}$* , Phys. Lett. **B313** (1993) 535.
- [27] A. De Angelis and L. Vitale, Nucl. Instrum. Meth. **A423** (1999) 446.